Supplemental Text for The multi-level analysis of *Arabidopsis* sepal growth reveals that cells are variable in timing of growth but not the maximum relative growth rate

Gerardo Tauriello, Heather M. Meyer, Richard S. Smith,
Petros Koumoutsakos, and Adrienne H. K. Roeder

This text extends the materials and method section of the main text and describes additional methods that were used to obtain the data shown.

1 Plant material, growth conditions and imaging

Growth and imaging of living sepals were conducted as described previously [2, 6]. Briefly, *Arabidopsis thaliana* plants of the Landsberg *erecta* accession expressing epidermal specific fluorescent nuclear marker pAR98 *ML1::H2B-mYFP* and epidermal specific plasma membrane fluorescent marker pAR169 *ML1::mCitrine-RCI2A* were grown on soil in 24 hour light conditions. After bolting, inflorescences were dissected to remove older flowers and expose the flower to be imaged. Plants were allowed to recover 6 hours after dissection before imaging. The whole plant was placed sideways on the microscope, the inflorescence was attached to a slide with tape, and the living flower was mounted in 0.02 % silwet 50 µg/ml Propidium Iodide (PI, Sigma P4170-10MG) under a cover slip. PI staining revealed damaged and dead cells. The same flower was imaged every 6 hours on a Zeiss 510 confocal microscope. Between images, the inflorescence was dried and the plant was returned to the growth chamber. YFP and mCitrine were excited with the 514 nm wavelength of an argon laser and fluorescent emission between 530 and 545 nm nm wavelengths was collected. PI was excited with the same 514 wavelength laser and the fluorescent emission between 585 and 615 was collected.

The original unprocessed images are available in the Bisque Image Browser on iPlant:
http://bovary.iplantcollaborative.org/client_service/browser?resource=/data_service/dataset

2 Function fitting and Akaike information criterion

Several places in our analysis required a fit of N data points $\{x_i, y_i\}$ to a function $f(x)$. The goal of the fit was to have $y_i \approx f(x_i)$ with an error, which is as small as possible. The function $f(x)$ depends on k parameters. If we use a function with too many parameters, we will overfit the data, while if we use too few parameters the error will be large. The error, which we try to

minimize, is given by the sum of squared errors (SSE):

$$SSE = \sum_i (f(x_i) - y_i)^2. \tag{1}$$

The quality of the fit is commonly reported with the coefficient of determination (R^2) and the root mean squared error $RMSE$, which are defined as:

$$R^2 = 1 - SSE/SST, \quad \text{where } SST = \sum_i \left(y_i - \sum_j y_j/N \right)^2, \tag{2}$$

$$RMSE = \sqrt{SSE/N}. \tag{3}$$

To compare different functions $f_j(x)$ with k_j free parameters, we use the corrected Akaike information criterion (AICc) [1]:

$$AIC_j = 2k_j + N \ln(SSE_j/N) + \frac{2k_j(k_j+1)}{N - k_j - 1}, \tag{4}$$

where SSE_j is the optimal value that we get after minimizing Eq. (1). The last term in Eq. (4) corrects for small sample sizes N. Functions $f_j(x)$ can be ranked according to AIC_j such that the best function is the one with the lowest AICc value ($AIC_{min} = \min_j(AIC_j)$). One can furthermore define the relative probability of each function as

$$r_j = \exp((AIC_{min} - AIC_j)/2), \tag{5}$$

such that function f_j is r_j times as likely as the best one. We can finally normalize Eq. (5) to obtain the probability p_j for each function f_j considered:

$$p_j = r_j / \sum_j r_j. \tag{6}$$

3 Uncertainty quantification and propagation

We expect our data to have unknown measurement and segmentation errors and we do not assume that our chosen function f is the perfect model when fitting data. The function f depends on parameters a_j ($j = 1, \ldots, k$). When we minimize the SSE (Eq. (1)) to obtain the best set of parameters, the function fitting introduces uncertainties in the parameters a_j, which are represented by the covariance matrix Σ. We compute Σ using the minimal value $SSE_m = \min_{\mathbf{a}}(SSE)$ and the Hessian $\mathbf{H}$ of SSE evaluated around the best set of parameters as

$$\Sigma = \frac{2SSE_m}{N}\mathbf{H}^{-1}, \quad H_{ij} = \frac{\partial^2 SSE}{\partial a_i \partial a_j}, \tag{7}$$

where N is the number of data points. The Hessian is either computed analytically (for linear functions f) or numerically using the `DERIVEST` toolbox in MATLAB [5].

We report uncertainties on quantities X by standard deviations σ_X which are either drawn as an error bar or reported as $X \pm \sigma_X$ wherever appropriate. If we assume the uncertainties to be normally distributed, we have a confidence of 68 % that the real value is within $X \pm \sigma_X$ and the 95 % confidence interval is given by $X \pm 1.96\,\sigma_X$. For the fitting parameters a_j, the standard deviations are given by the square root of the diagonal entries of Σ.

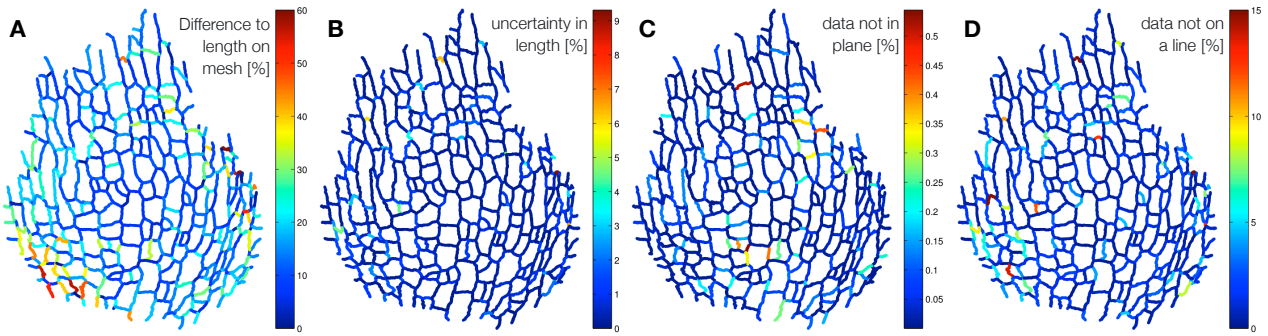

Figure M1: Assessment of wall length correction shown for Flower B. We show the difference with respect to the length measured on the mesh (A), the uncertainty in the length, the amount of data which is not on a plane (C) and the amount of data which cannot be described with a straight line (D). All quantities are shown in [%].

When we compute derived quantities, we determine the corresponding standard deviations by propagating the uncertainty of the fit. Any derived quantity can be written as a function $g(a_1, \ldots, a_k)$ for which we wish to compute the standard deviation σ_g. We can approximate σ_g by computing the variance of the quantity g as $\sigma_g^2 = J_g \, \Sigma \, J_g^T$, where $J_g = \nabla g$ is the Jacobian of g. This approximation is exact for linear functions and has been shown to be well suited for nonlinear functions as well [7].

4 Image processing

We implemented a scheme to measure wall lengths more accurately by assuming a smooth wall segment shape (Fig. S1F and Fig. M1). The corrected wall length can differ considerably with respect to the length measured on the mesh (up to 60 % shown in Fig. M1A and more observed at later time points). We can measure the uncertainty of the corrected wall length and we usually obtain uncertainties well below 10 % (Fig. M1B). Wall lengths with uncertainties larger than 10 % are filtered out from our analysis. To obtain the corrected wall lengths, we first perform a principal component analysis (PCA) to project all mesh vertices of a wall segment onto a plane. The amount of out-of-plane data is usually below 1 % (Fig. M1C). The amount of data which cannot be explained with a straight line on the other hand can be above 10 % (Fig. M1D and more at later time points). The vertices which were projected onto the principal plane are finally fitted to a quadratic function and the corrected wall length is given by the length of the parabola. The uncertainty of the corrected wall length is propagated from the uncertainty of the fit to a quadratic function.

Additionally to cell areas and wall segment lengths, we also extracted the center and surface normal of each cell and the center and principal direction of each wall segment in 3D on the curved surface. We furthermore compute the angle between a top-bottom axis defined in the sepal and the principal direction of each cell and wall segment (Fig. M2). The angles are computed by performing separate PCAs for the whole sepal, for each cell and for each wall segment. The PCA for the whole sepal is used to project the 3D data to 2D by removing the third component of the PCA. The principal direction for each cell and wall segment is given by the first component of the corresponding PCA. We observe that the cells (especially the larger ones) are commonly aligned with the top-bottom axis of the sepal. We therefore average the principal direction of all cells weighted by their area to obtain the top-bottom axis of the sepal. The angles between this top-bottom axis and the principal directions of cells and wall segments were measured within the two dimensional projection of the sepal. This is done to

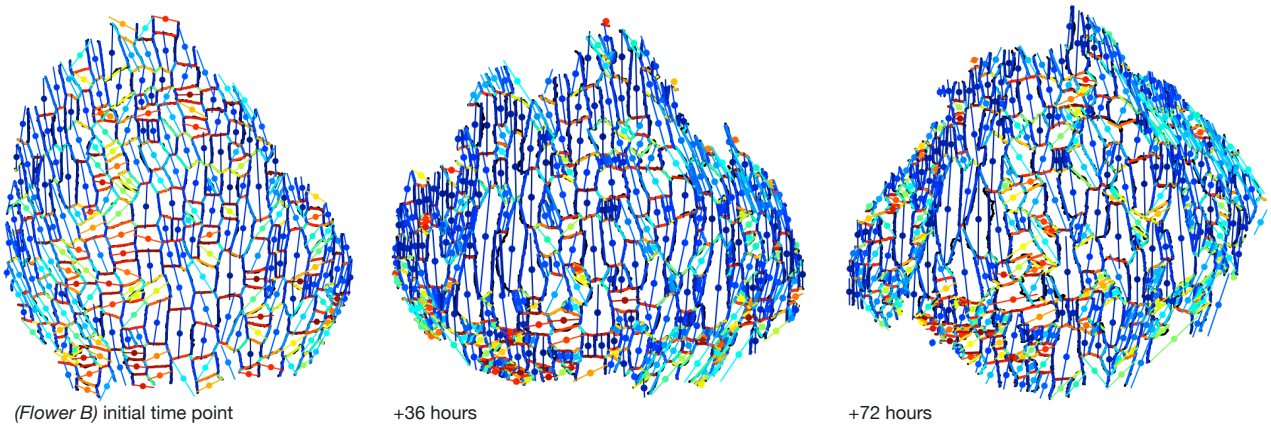

Figure M2: Principal directions for walls and cells for Flower B at an initial time point and after 36 and 72 hours (left to right). The sepals are rotated such that the y-axis corresponds to a top-bottom axis and rescaled to have the same height. The principal directions are shown as lines and are colored according to their angle with respect to the top-bottom axis (blue = parallel, red = orthogonal).

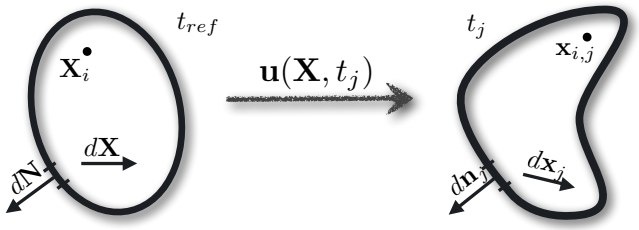

Figure M3: We approximate continuous low-order displacement fields $\mathbf{u}(\mathbf{X}, t_j)$ to map each point $\mathbf{X} = \mathbf{X}_i$ of the sepal at a reference time point t_{ref} to its location $\mathbf{x}_{i,j}$ at any other time point t_j. The field $\mathbf{u}(\mathbf{X}, t_j)$ is used to compute changes of vectors $d\mathbf{X}$ and surface elements $d\mathbf{N}$.

avoid measuring angles due to the curvature of the sepal.

5 Continuous deformation field

We use the tracking of cells and wall segments to define continuous low-order displacement fields $\mathbf{u}(\mathbf{X}, t_j)$ between a reference time point t_{ref} and any other discrete time point t_j (Fig. M3). The fields $\mathbf{u}(\mathbf{X}, t_j)$ filter out spatial variability and enable the observation of growth averaged over regions of the tissue. We can estimate the deformation of line elements $d\mathbf{X}$ and area elements $d\mathbf{N}$ (Fig. M3) using the deformation gradient $\mathbf{F_j}(\mathbf{X}) = \mathbf{I} + \partial \mathbf{u}(\mathbf{X}, t_j)/\partial \mathbf{X}$ [4]. Each line element (such as a wall segment) at time t_{ref} has a length $L_{ref} = \|d\mathbf{X}\|$ and a direction $d\mathbf{X}/L_{ref}$. Area elements (such as cell areas) are defined by an area $A_{ref} = \|d\mathbf{N}\|$ and a surface normal $d\mathbf{N}/A_{ref}$. We predict line elements $d\mathbf{x}_j$ and area elements $d\mathbf{n}_j$ at time point t_j by computing $d\mathbf{x}_j = \mathbf{F_j}\, d\mathbf{X}$ and $d\mathbf{n}_j = \det(\mathbf{F_j})\, \mathbf{F_j^{-T}} d\mathbf{N}$ respectively. The predicted length and area are then given by $L_j = \|d\mathbf{x}_j\|$ and $A_j = \|d\mathbf{n}_j\|$, respectively. In addition to the "real data" from the segmented images, we use these formulas to generate "avg. data" for the time evolution of cell areas and wall segment lengths. The avg. data is expected to filter out spatial variability both due to segmentation errors and due to real differences between neighboring cells.

We consider the centers of each cell and wall segment shared between the time points t_j and t_{ref} as landmark points. Each landmark point i has a position $\mathbf{X}_i$ at time t_{ref} and $\mathbf{x}_{i,j}$ at time t_j. Given a functional form for $\mathbf{u}(\mathbf{X}, t_j)$, which we choose to be polynomial, we find the parameters by minimizing the SSE, which in this case is given by $SSE = \sum_i \|\mathbf{x}_{i,j} - \mathbf{X}_i - \mathbf{u}(\mathbf{X}_i, t_j)\|^2$.

To test the plausibility of having uniform growth we change the function to be minimized to additionally enforce a constant relative change in cell area. Given the displacement field $\mathbf{u}(\mathbf{X}, t_j)$, we can compute the relative area change with the formulas above and get a predicted area change $A_{k,j}$ for each cell k at time t_j. We then minimize the function

$$f(\mathbf{a}) = \frac{w}{N_L} SSE + \frac{1}{N_C} \sum_k \left(A_{k,j} - \frac{1}{N_C} \sum_l A_{l,j} \right)^2, \quad w = 10^{-3}/L^2, \quad L = \sqrt{\frac{\sum_i \|\mathbf{X}_i\|^2}{3N_C}}, \tag{8}$$

where $\mathbf{a}$ is the set of parameters that determine $\mathbf{u}(\mathbf{X}, t_j)$, N_L is the number of landmark points, N_C is the number of cells, w is a weighting factor and L is a length scale, which depends on the data. The additional term in Eq. (8) essentially forces the variance of $A_{k,j}$ to be zero and hence enforces uniform growth. The function $f(\mathbf{a})$ is harder to minimize than SSE and we employ a MATLAB implementation of the CMA-ES [3] algorithm to minimize $f(\mathbf{a})$.

6 Growth curves

6.1 Definition of growth curves

We define growth curves for all cells and wall segments i existing at the reference time point t_{ref}. We consider cell areas $A_{i,j}$ and wall segment lengths $L_{i,j}$ at time points t_j. We normalize the sizes with respect to the area $A_{i,ref}$ and the length $L_{i,ref}$ at the reference time point t_{ref} to obtain the growth curves $\tilde{A}_{i,j} = A_{i,j}/A_{i,ref}$ and $\tilde{L}_{i,j} = L_{i,j}/L_{i,ref}$.

We analogously define globally averaged growth curves. We compute the globally averaged areas $\tilde{A}^G_j$ and lengths $\tilde{L}^G_j$ by adding up all shared cells and walls as

$$\tilde{A}^G_j = \sum_{k \in \mathcal{C}_j} A_{k,j} / \sum_{k \in \mathcal{C}_j} A_{k,ref}, \quad \tilde{L}^G_j = \sum_{k \in \mathcal{W}_j} L_{k,j} / \sum_{k \in \mathcal{W}_j} L_{k,ref}, \tag{9}$$

where $\mathcal{C}_j$ and $\mathcal{W}_j$ are the sets of all shared cells and walls between time points t_j and t_{ref}. The shared cells may also contain cell lineages while wall lineages are not considered. We define the globally averaged areas $\tilde{A}^G_j$ as "tissue growth curve" in the main text as it includes all segmented and tracked cells and it is therefore equivalent to computing a growth curve for the whole tissue. We furthermore compute $\tilde{A}^{Gd}_j$ and $\tilde{A}^{Gn}_j$ which are defined as $\tilde{A}^G_j$ but only consider dividing and non-dividing cells respectively. We define "non-dividing" cells as cells, which did not divide within the time period of observation. These are commonly giant cells but may also include cells, which divide after the last observed time point.

6.2 Function fitting

To compare the growth curves, we compute statistics based on fitting a sigmoid (S) curve to the data. We use a shifted logistic function (Fig. 8C) with four degrees of freedom defined as

$$f(t) = \frac{a}{1 + \exp(k\,(t_m - t))} + b. \tag{10}$$

The curve is motivated by observations from the globally averaged growth curves and from individual growth curves. We clearly see a flattening of the growth rates which could not be captured with an exponential growth model. At early stages of growth the sigmoid curve

resembles an exponential, close to $t = t_m$ it looks like a linear function and at late stages it flattens like an exponentially saturating curve. We furthermore compared the S curve with two alternatives: an exponential ($f(t) = a\exp(k\,t)$), which has a constant relative growth rate ($f'/f = k$) and a linear function ($f(t) = a + b\,t$), which has a constant growth rate ($f' = b$). A comparison based on the quality of the fit (R^2 and $RMSE$) and the Akaike information criterion (as defined in §2) revealed that the S curve is the most probable model to define growth curves for the given data (Fig. 8, 9, S2, S13, S14).

We perform the function fitting with a constrained ($\{a, b, k\} \geq 0$) optimization routine in MATLAB (`fmincon`) [5]. For each cell i we take the data points $A_{i,j}$ at time points t_j and we find the parameters (a, b, k, t_m) for which the SSE $\sum_j (f(t_j) - A_{i,j})^2$ is minimal. The same is done for each wall segment i with lengths $L_{i,j}$. We perform this procedure for the global growth curves as well as for the individual growth curves of both the "real data" and the "avg. data" generated with the low-order displacement fields. Keep in mind that for each growth curve, we expect to get a different set of parameters. We also keep track of the uncertainty of the fit by storing the covariance matrix Σ which relates the errors in the parameters (a, b, k, t_m) and use it to define error bars and confidence intervals as defined in §3.

We report a and b as dimensionless numbers, k in units of [1/h] and t_m in units of [h]. Given the parameters from fitting the shifted logistic function, we compute the growth rate $\mathrm{GR}(t) = df/dt$ and the relative growth rate $\mathrm{RGR}(t) = \mathrm{GR}(t)/f(t)$. The growth rate $\mathrm{GR}(t)$ defines how fast cell area or wall length increases in time while the relative growth rate $\mathrm{RGR}(t)$ defines the relative increase in cell area or wall length and is given in units of [1/h]. The relative growth rate reaches its maximum at $t = t_x = t_m - \ln((a + b)/b)/(2k)$ and we report t_x in units of [h]. When comparing the growth rate with the size of cells and walls at $t = t_m$ and $t = t_x$ (Fig. 1, 11, S3, S16), we report the cell area as $A_{i,r}\,f(t)$ (in units of [μm^2]), the wall length as $L_{i,r}\,f(t)$ (in units of [μm]), the growth rate for cells as $A_{i,r}\,\mathrm{GR}(t)$ (in units of [μm^2/h]) and the growth rate for walls as $L_{i,r}\,\mathrm{GR}(t)$ (in units of [μm/h]).

6.3 Results for globally averaged growth curves

We show the globally averaged growth curves with the corresponding sigmoid fits for all flowers (Fig. M4). We analyzed area growth considering all cells ($\tilde{A}_j^G$, red), only non-dividing cells ($\tilde{A}_j^{Gn}$, purple) and only dividing cells ($\tilde{A}_j^{Gd}$, green). The wall length change ($\tilde{L}_j^G$, blue) was computed considering walls that did not divide since or until the reference time point. We see that cell division did not have a major influence on the growth curves during the stages observed.

The fit to the sigmoid curve was essentially perfect with a coefficient of determination $R^2 > 0.996$ in all cases. We report the fitting parameters (a, b, k, t_m) and t_x in Table 1. We note that t_x is undefined if $b = 0$ and that b is hard to estimate (large uncertainties) if our data is at a late stage of development (e.g. Flower B), while a and t_m are hard to estimate if we only see the early stages of development (e.g. Flower D).

6.4 Growth curves with meaningful fits

It is important for the fitting procedure that we have a reasonably large number of observations and we usually drop results with less than 8 of them. It is also required that we have data for the later stages of growth (at least until t_m) to have a meaningful fit. Otherwise, the uncertainties in the fitting parameters prevent a further investigation of the growth curve. In

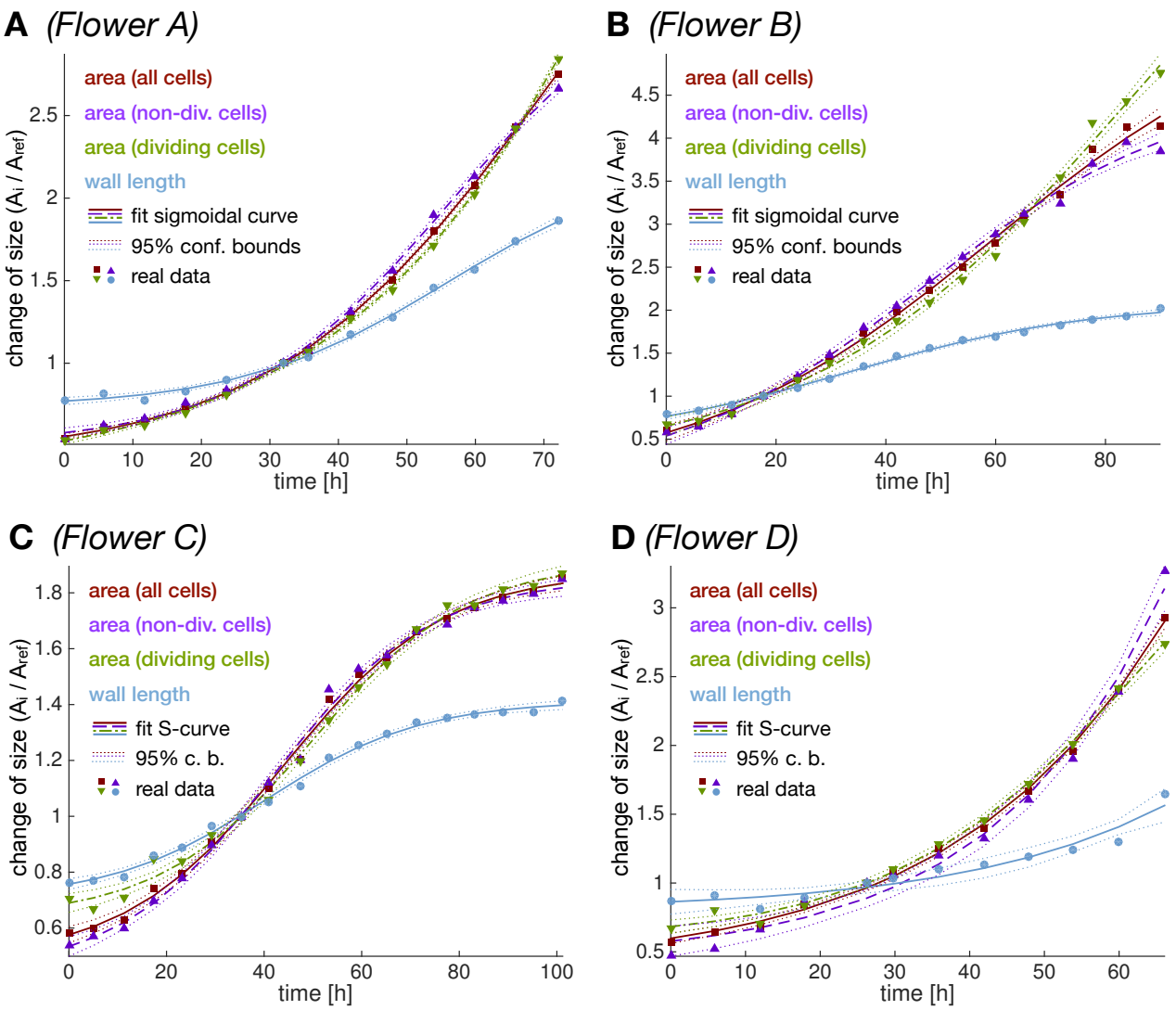

Figure M4: Globally averaged growth curves fit sigmoid shapes. We show global changes of cell area and wall length with respect to the reference time point for Flowers A (A), B (B), C (C) and D (D). We computed the area change considering all cells (red), only non-dividing cells (purple) and only dividing cells (green). The wall length change (blue) at each time point was computed considering walls that did not divide since or until the reference time point. We show the fit to a logistic function as solid lines, the 95 % confidence interval as dotted lines and the data as markers.

Table 1: Fitting parameters (a, b, k, t_m) and t_x for globally averaged growth curves based on a fit to a sigmoid curve for all flowers. We report quantities with standard deviations propagated from the uncertainty of the fit.

	flower	area (all cells)	area (non-div. cells)	area (div. cells)	length (non-div. walls)
a	A	4.51 ± 0.365	2.94 ± 0.173	16.7 ± 6.41	1.5 ± 0.123
b	A	0.427 ± 0.0226	0.507 ± 0.0267	0.316 ± 0.0316	0.735 ± 0.0195
k [1/h]	A	0.05 ± 0.00252	0.0654 ± 0.00416	0.0364 ± 0.00217	0.0667 ± 0.00597
t_m [h]	A	70.7 ± 2.84	56.4 ± 1.6	119 ± 14.7	55.8 ± 2.23
t_x [h]	A	46.2 ± 0.822	41.7 ± 0.788	64.7 ± 5.56	47.5 ± 1.25
a	B	5.66 ± 0.68	4.61 ± 0.414	8.49 ± 2.06	1.62 ± 0.15
b	B	0 ± 0.213	0 ± 0.201	0.204 ± 0.207	0.471 ± 0.105
k [1/h]	B	0.0366 ± 0.00517	0.0426 ± 0.00529	0.0342 ± 0.00607	0.0452 ± 0.00563
t_m [h]	B	59.7 ± 3.68	47.5 ± 1.92	84.4 ± 11.7	33.2 ± 2.34
t_x [h]	B	-	-	29.5 ± 17.1	16.8 ± 6.65
a	C	1.39 ± 0.0477	1.41 ± 0.0547	1.27 ± 0.0509	0.709 ± 0.0302
b	C	0.487 ± 0.0317	0.439 ± 0.0381	0.639 ± 0.0298	0.704 ± 0.022
k [1/h]	C	0.061 ± 0.00391	0.063 ± 0.00458	0.0634 ± 0.005	0.0625 ± 0.00482
t_m [h]	C	44 ± 0.927	41.8 ± 1.06	50.1 ± 1.07	40.3 ± 1.23
t_x [h]	C	32.9 ± 1.88	30.4 ± 2.28	41.4 ± 1.67	34.7 ± 1.73
a	D	33.6 ± 8.73	57.1 ± 47.1	4.34 ± 1.06	12.5 ± 11.8
b	D	0.382 ± 0.0453	0.443 ± 0.0987	0.578 ± 0.0573	0.805 ± 0.112
k [1/h]	D	0.0382 ± 0.00198	0.0461 ± 0.00545	0.056 ± 0.00797	0.0395 ± 0.0171
t_m [h]	D	132 ± 9.37	131 ± 22.3	66.1 ± 7.65	135 ± 47.1
t_x [h]	D	73.1 ± 3.79	78.5 ± 9.99	47 ± 2.84	99.8 ± 22.3

the main text, we account for the uncertainties in the fitting parameters and only report curves with a meaningful fit. A meaningful fit is only given if: we had enough data points (≥ 8), the fitting procedure converged to an optimum, the fit was good enough ($R^2 > 0.9$) and the uncertainty in the fitting parameters was low ($\sigma_k/k^2 < 11$ h).

6.5 Observations on S curves

A few interesting observations can be made for the S curve defined in Eq. (10). The growth rate $\mathrm{GR}(t)$ reaches its maximum at $t = t_m$ with $\mathrm{GR}(t_m) = ak/4$. The relative growth rate $\mathrm{RGR}(t)$, on the other hand, is maximal at $t = t_x = t_m - \ln(r)/(2k)$ with $\mathrm{RGR}(t_x) = k(\sqrt{r}-1)/(\sqrt{r}+1)$, where we introduced $r = (a+b)/b$, which is the ratio of the initial ($t \to -\infty$) and final ($t \to \infty$) sizes $f(t)$. Furthermore, $\mathrm{RGR}(t)$ is symmetric around t_x:

$$\mathrm{RGR}(t_x + \hat{t}) = \frac{k\,(r-1)}{\left(1+\sqrt{r}\exp(-\hat{t}k)\right)\left(1+\sqrt{r}\exp(\hat{t}k)\right)}. \tag{11}$$

One can immediately see in Eq. (11) that $\mathrm{RGR}(t_x + \hat{t}) = \mathrm{RGR}(t_x - \hat{t})$.

In the main text, we showed that we could collapse $f_c(\hat{t}) = f(t_m + \hat{t})/f(t_m)$. One can show that $f_c(\hat{t})$ is indeed expected to collapse to a single curve if $f(t)$ is defined as in Eq. (10) and if all lineages have the same constant values for $\mathrm{RGR}(t_x)$ and $\mathrm{RGR}(t_m)$. First we write $f_c(\hat{t})$,

$\mathrm{RGR}(t_x)$ and $\mathrm{RGR}(t_m)$ as functions of r and k:

$$f_c(\hat{t}) = \frac{f(t_m + \hat{t})}{f(t_m)} = \frac{2\left(1 + r\exp(\hat{t}k)\right)}{\left(1 + \exp(\hat{t}k)\right)(1 + r)}, \tag{12}$$

$$\mathrm{RGR}(t_x) = \frac{k\left(\sqrt{r} - 1\right)}{\sqrt{r} + 1}, \tag{13}$$

$$\mathrm{RGR}(t_m) = \frac{k\left(r - 1\right)}{2\left(r + 1\right)}. \tag{14}$$

If all cell lineages have the same constant values $c_x = \mathrm{RGR}(t_x)$ and $c_m = \mathrm{RGR}(t_m)$, we can therefore solve Eq. (13-14) for the unknown r and k. Since $f_c(\hat{t})$ in Eq. (12) only depends on r and k, all cell lineages are then expected to have the same $f_c(\hat{t})$.

References

[1] K. P. Burnham and D. R. Anderson. *Model Selection and Multimodel Inference: A Practical Information-Theoretic Approach*. Springer, New York, 2nd edition, 2002.

[2] A. Cunha, P. T. Tarr, A. H. K. Roeder, A. Altinok, E. Mjolsness, E. M. Meyerowitz, A. R. Asthagiri, and A. P. Arkin. Computational analysis of live cell images of the Arabidopsis thaliana plant. In *Methods Cell Biol.*, volume 110, pages 285–323. Academic Press, 2012.

[3] N. Hansen, S. Müller, and P. Koumoutsakos. Reducing the time complexity of the derandomized evolution strategy with covariance matrix adaptation (CMA-ES). *Evol. Comput.*, 11(1):1–18, Mar. 2003.

[4] P. Howell, G. Kozyreff, and J. Ockendon. *Applied Solid Mechanics*. Cambridge University Press, Cambridge, 2009.

[5] MATLAB. *version R2015a*. The MathWorks Inc., Natick, Massachusetts, 2012.

[6] A. H. K. Roeder, V. Chickarmane, A. Cunha, B. Obara, B. S. Manjunath, and E. M. Meyerowitz. Variability in the control of cell division underlies sepal epidermal patterning in Arabidopsis thaliana. *PLOS Biol.*, 8(5):e1000367, 2010.

[7] J. Tellinghuisen. Statistical error propagation. *J. Phys. Chem. A*, 105(15):3917–3921, Feb. 2001.